

# GALEX: Galaxy Evolution Explorer

Barry F. Madore

*Carnegie Observatories, Pasadena CA 91101, e-mail: barry@ociw.edu*

**Abstract.** We review recent scientific results from the Galaxy Evolution Explorer with special emphasis on star formation in nearby resolved galaxies.

## INTRODUCTION

### The Satellite

The Galaxy Evolution Explorer (GALEX) is a NASA Small Explorer class mission. It consists of a 50 cm-diameter, modified Ritchey-Chrétien telescope with four operating modes: Far-UV (FUV) and Near-UV (NUV) imaging, and FUV and NUV spectroscopy. The telescope has a 3-m focal length and has Al-MgF<sub>2</sub> coatings. The field of view is 1.2° circular. An optics wheel can position a CaF<sub>2</sub> imaging window, a CaF<sub>2</sub> transmission grism, or a fully opaque mask in the beam. Spectroscopic observations are obtained at multiple grism-sky dispersion angles, so as to mitigate spectral overlap effects. The FUV (1528Å: 1344-1786Å) and NUV (2271Å: 1771-2831Å) imagers can be operated one at a time or simultaneously using a dichroic beam splitter. The detector system incorporates sealed-tube microchannel-plate detectors. The FUV detector is preceded by a blue-edge filter that blocks the night-side airglow lines of OI1304, 1356, and Ly $\alpha$ . The NUV detector is preceded by a red blocking filter/fold mirror, which produces a sharper long-wavelength cutoff than the detector CsTe photocathode and thereby reduces both zodiacal light background and optical contamination. The peak quantum efficiency of the detector is 12% (FUV) and 8% (NUV). The detectors are linear up to a local (stellar) count-rate of 100 (FUV), 400 (NUV) cps, which corresponds to  $m_{AB} \sim 14 - 15$ . The resolution of the system is typically 4.5/6.0 (FUV/NUV) arcseconds (FWHM), and varies by  $\sim 20\%$  over the field of view. Further detail about the mission, in general, and the performance of the satellite, in specific, can be found in Martin *et al.* [6] and Morrissey *et al.* [7], respectively. The mission is nominally expected to last 38 months; GALEX was launched into a 700 km, 29° inclination, circular orbit on 28 April 2003.

**TABLE 1.** Selected Performance Parameters (Morrissey *et al.* 2005)

Item	FUV Band	NUV Band
Bandwidth:	1344 – 1786 Å	1771 – 2831 Å
Effective wavelength ( $\lambda_{\text{eff}}$ ):	1528 Å	2271 Å
Field of view:	1.28°	1.24°
Zero point ( $m_0$ ):	18.82 mag	20.08 mag
Image resolution (FWHM):	4.5 arcsec	6.0 arcsec
Spectral resolution ( $\lambda/\Delta\lambda$ ):	200	90
Detector background (typical):		
Total:	78 c-sec <sup>-1</sup>	193 c-sec <sup>-1</sup>
Diffuse:	0.66 c-sec <sup>-1</sup> ·cm <sup>-2</sup>	1.82 c-sec <sup>-1</sup> ·cm <sup>-2</sup>
Hotspots:	47 c-sec <sup>-1</sup>	107 c-sec <sup>-1</sup>
Sky background (typical):	2000 c-sec <sup>-1</sup>	20000 c-sec <sup>-1</sup>
Limiting magnitude (5 $\sigma$ ):		
AIS (100 sec):	19.9 mag	20.8 mag
MIS (1500 sec):	22.6 mag	22.7 mag
DIS (30000 sec):	24.8 mag	24.4 mag

## The Prime Mission

GALEX is currently undertaking the first space UV sky-survey, including both imaging and grism surveys. The prime mission includes an all-sky imaging survey (AIS: 75-95% of the observable sky, subject to bright-star and diffuse Galactic background light limits) ( $m_{AB} \simeq 20.5$ ), a medium imaging survey (MIS) of  $1000 \text{ deg}^2$  ( $m_{AB} \simeq 23$ ), a deep imaging survey (DIS) of 100 square degrees ( $m_{AB} \simeq 25$ ), and a nearby galaxy survey (NGS). Spectroscopic (slitless) grism surveys ( $R=100-200$ ) are also being undertaken with various depths and sky coverage. Many of the GALEX fields overlap existing and/or planned ground-based and space-based surveys being undertaken in other bands.

*All-sky Imaging Survey (AIS):* The goal of the AIS is to survey the entire sky subject to a sensitivity of  $m_{AB} \simeq 20.5$ , comparable to the POSS II ( $m_{AB}=21$  mag) and SDSS spectroscopic ( $m_{AB}=17.6$  mag) limits. Several hundred to 1,000 objects are in each  $1 \text{ deg}^2$  field. The AIS is performed in roughly ten 100-second pointed exposures per eclipse ( $\sim 10 \text{ deg}^2$  per eclipse).

*Medium Imaging Survey (MIS):* The MIS covers  $1000 \text{ deg}^2$ , with extensive overlap of the Sloan Digital Sky Survey. MIS exposures are a single eclipse, typically 1500 seconds, with sensitivity  $m_{AB} \simeq 23$ , net several thousand objects, and are well-matched to SDSS photometric limits.

Bianchi *et al.* [1] have made the first characterization of the objects detected in the GALEX AIS and DIS surveys by cross-comparing objects already discovered and classified on the Sloan Digital Sky Survey in regions of overlap. Emphasis was put on discovering quasars and for the 75 and 92 square degrees studied in the MIS and AIS overlap with SDSS they report 1,736 and 222  $z \leq 2$  QSO candidates, for the two GALEX survey depths, respectively. This significantly increases the number of fainter candidates, and moderately augments the candidate list for brighter objects.

*Deep Imaging Survey (DIS):* The DIS consists of 20 orbit (30 ksec,  $m_{AB} \simeq 25$ ) exposures, over  $80 \text{ deg}^2$ , located in regions where major multiwavelength efforts are already underway. DIS regions have low extinction, low zodiacal and diffuse galactic backgrounds, contiguous pointings of  $10 \text{ deg}^2$  to obtain large cosmic volumes, and minimal bright stars. An Ultra DIS of 200 ksec,  $m_{AB} \sim 26$  mag is also in progress in four fields.

*Nearby Galaxies Survey (NGS):* The NGS targets well-resolved nearby galaxies for 1-2 eclipses. Surface brightness limits are  $m_{AB} \sim 27.5$  mag  $\text{arcsec}^{-2}$ . The 200 targets are a diverse selection of galaxy types and environments, and include most galaxies from the Spitzer IR Nearby Galaxy Survey (SINGS). Figure 1 shows the NGS observation of the M81/M82 system.

*Spectroscopic Surveys.* The suite of spectroscopic surveys includes (1) the Wide-field Spectroscopic Survey (WSS), which covers the full  $80 \text{ deg}^2$  DIS footprint with comparable exposure time (30 ksec), and reaches  $m_{AB} \sim 20$  mag for  $S/N \sim 10$  spectra; (2) the Medium Spectroscopic Survey (MSS), which covers the high priority central field in each DIS survey region (total  $8 \text{ deg}^2$ ) to  $m_{AB} = 21.5\text{--}23.0$  mag, using 300 ksec exposures; and (3) Deep Spectroscopic Survey (DSS) covering  $2 \text{ deg}^2$  with 1,000 eclipses, to a depth of  $m_{AB} = 23\text{--}24$  mag.

## NEARBY GALAXY SURVEY (NGS)

### NGC 0253 and M82

In a study of the complex of ultraviolet filaments in the starburst-driven halos of NGC 0253 and M82 Hoopes *et al.* [5] concluded that the UV luminosities in the halo are too high to be provided by continuum and line emission from shock-heated or photoionized gas except perhaps in the brightest filaments in M82. This suggests that most of the UV light is the stellar continuum of the starburst scattered into our line of sight by dust in the outflow. This interpretation agrees with previous results from optical imaging polarimetry in M82. The observed luminosity of the halo UV light is  $\leq 0.1\%$  of the bolometric luminosity of the starburst. The morphology of the UV filaments in both galaxies shows a high degree of spatial correlation with H $\alpha$  and X-ray emission, which indicates that these outflows contain cold gas and dust, some of which may be vented into the intergalactic medium (IGM). UV light is seen in the “H $\alpha$  cap” 11 kpc north of M82. If this cap is a result of the wind fluid running into a pre-existing gas cloud, the gas cloud contains dust and is not primordial in nature but was probably stripped from M82 or M81 (Figure 2). If starburst winds efficiently expel dust into the IGM, this could have significant consequences for the observation of cosmologically distant objects.

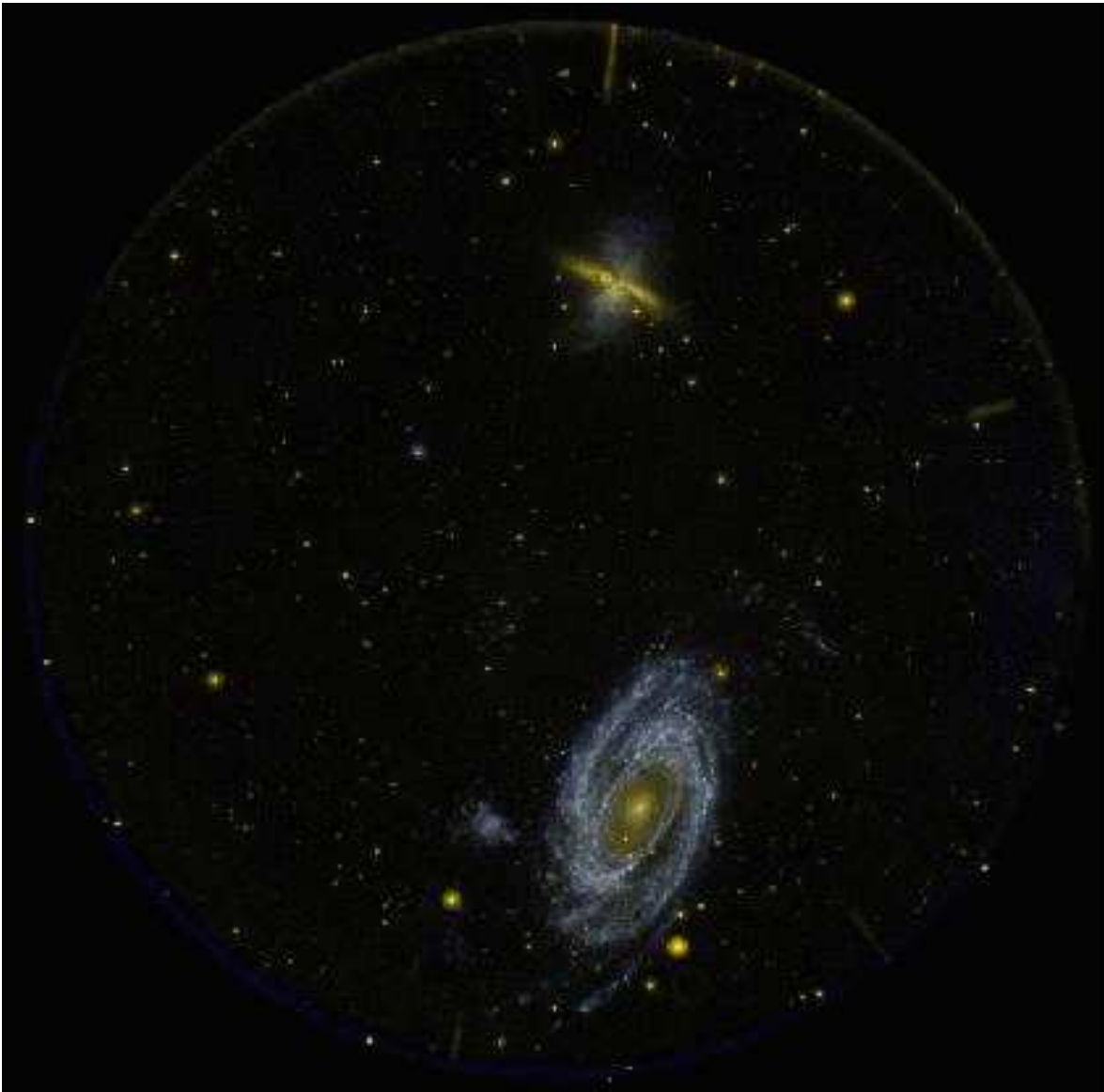


**FIGURE 1.** GALEX Composite NUV/FUV Image of M81 (bottom) and M82 (top). Note the very different morphology of M82 as compared to its optical image. The scattering of light by dust ejected by the starburst is especially prominent in the blue light detected by GALEX. On the other hand, the bulge of M81 is almost invisible in the GALEX bands, leaving only the complex array of star-forming filaments detailing the spiral structure of this galaxy. The irregular object to the east of M81 is Holmberg IX. Another interacting galaxy in the M81-M82 system, NGC 3077 is outside the field of view to the east and may never be imaged by GALEX because of a nearby bright star.

### M31, M32 and M33: Radial Gradients

For M31 and M33 (Figures 3 & 4, respectively) Thilker *et al.* [13] have determined the UV radial light and color profiles and compared them with the distribution of ionized gas as traced by H $\alpha$  emission. It is found that the extent of the UV emission, in both

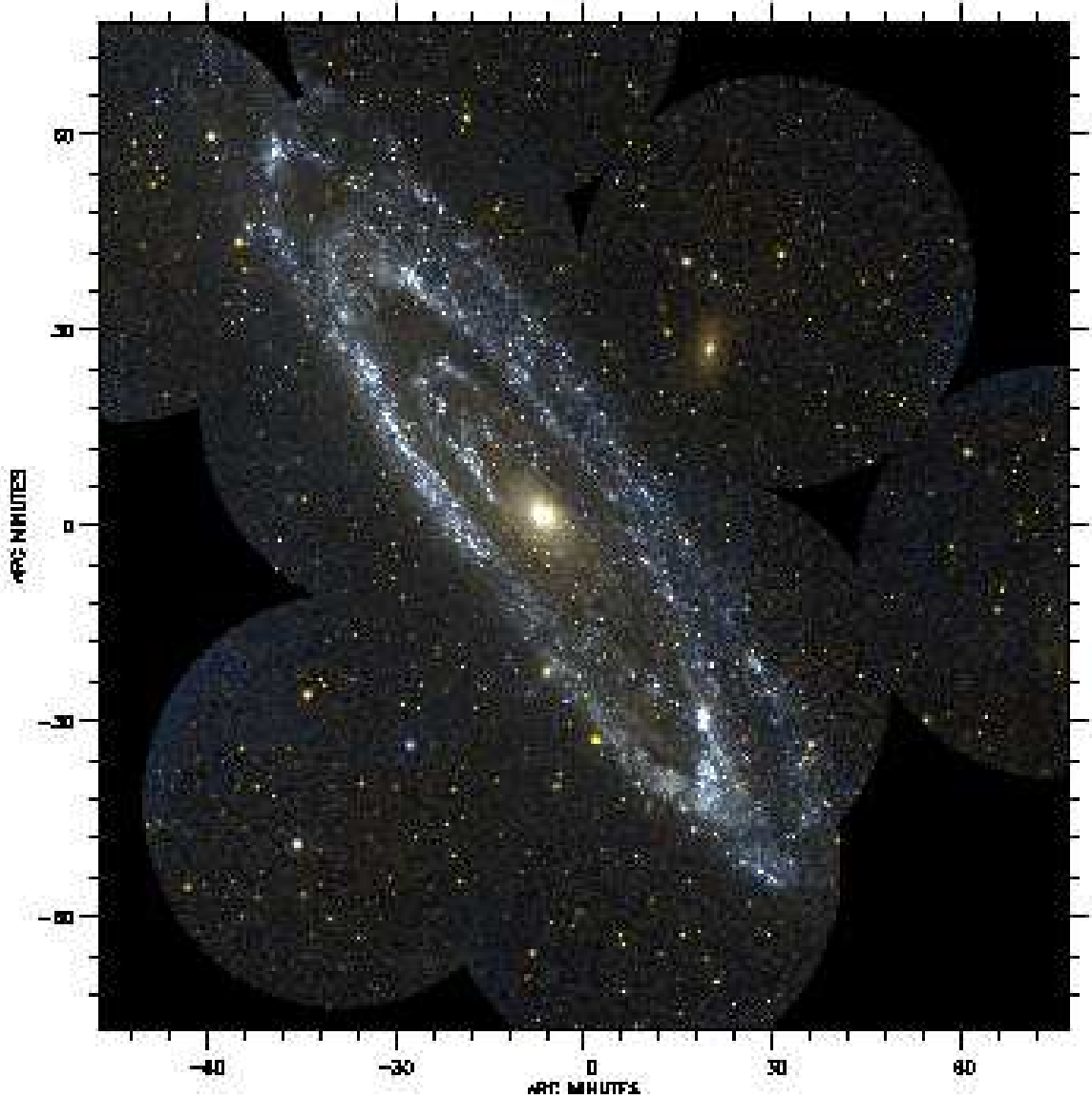


**FIGURE 2.** GALEX Montage of M31. As large as the field of view of GALEX is, it still requires many pointings (in this case 9 images) to cover the main body of the galaxy and part of its halo. Both M32 and NGC 205 are visible in this image, but because of their intrinsically red population they are not as conspicuous as they are in the visible.

targets, is greater than the extent of the observed  $HII$  regions and diffuse ionized gas. In addition, the ultraviolet diffuse fraction in M33 using the FUV observations has been compared to the  $H\alpha$  diffuse fraction obtained from wide-field narrow-band imaging. The FUV diffuse fraction appears to be remarkably constant near 0.65 over a large range in galactocentric radius, with departures to higher values in circumnuclear regions and, most notably, at the limit of the  $H\alpha$  disk. The authors suggest that the increase in FUV diffuse fraction at large galactocentric radii could indicate that a substantial

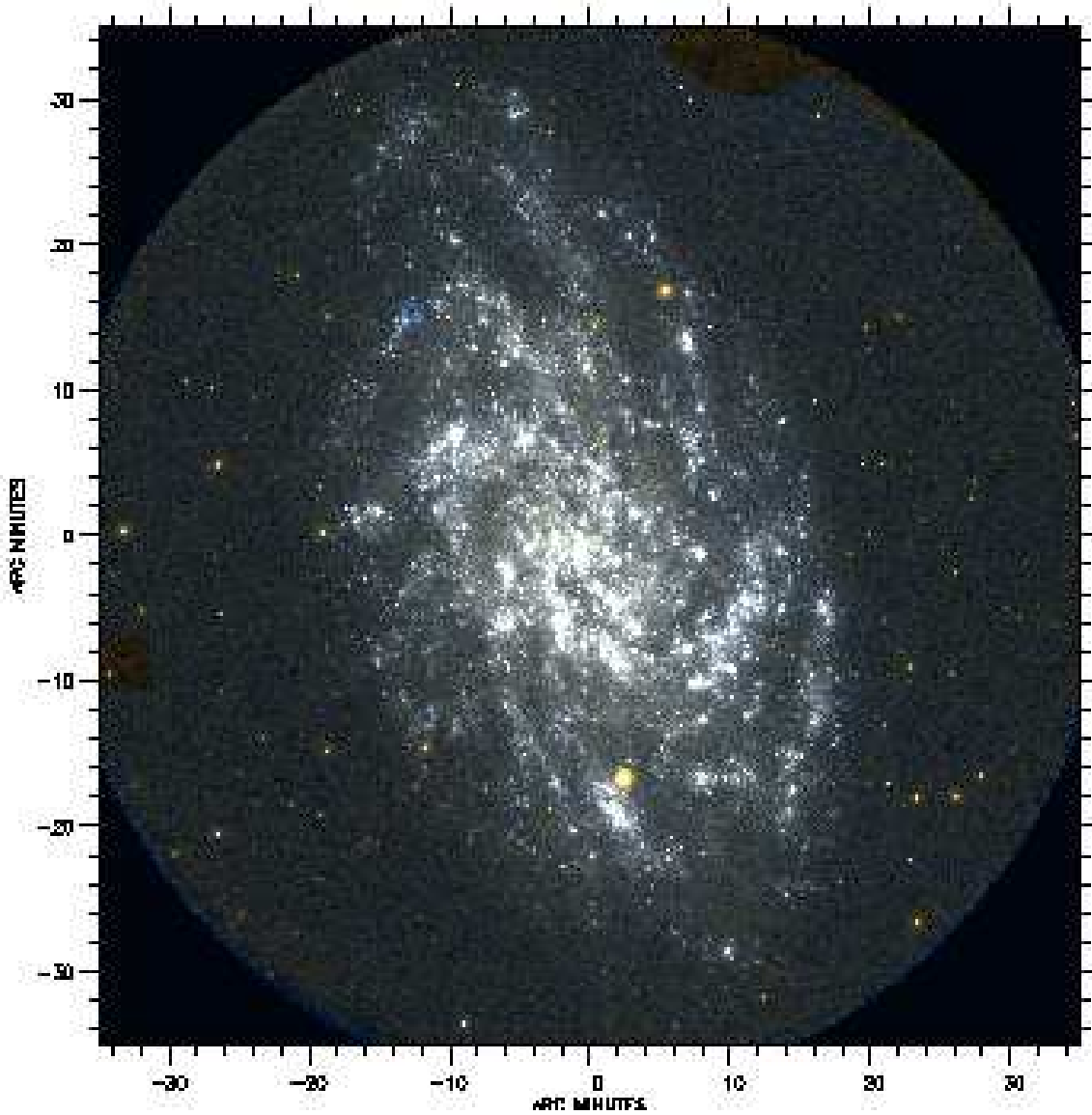


**FIGURE 3.** GALEX Montage of M33. A single pointing of GALEX is capable of imaging almost the entire main body of M33. Because M33 has only a faint background population of old red stars its morphology in the UV is not too dissimilar to its appearance at the optical wavelengths. The primary difference being the contrast of the arms with respect to the disk.

portion of the diffuse emission beyond this point is not generated *in situ* but rather it is scattered from dust, after originating in the vicinity of the disk's outermost *HII* regions. A radial variation of the  $H\alpha$  diffuse fraction was also measured: in general the  $H\alpha$  diffuse fraction is near 0.4 but it rises up to 0.6 toward the galaxy center.

For M32, the high-surface-brightness elliptical companion to the Andromeda galaxy, Gil de Paz *et al.* [12] have undertaken a detailed analysis of its UV light and color profile. Early studies of the UV properties of this galaxy, first by O'Connell *et al.* [9]

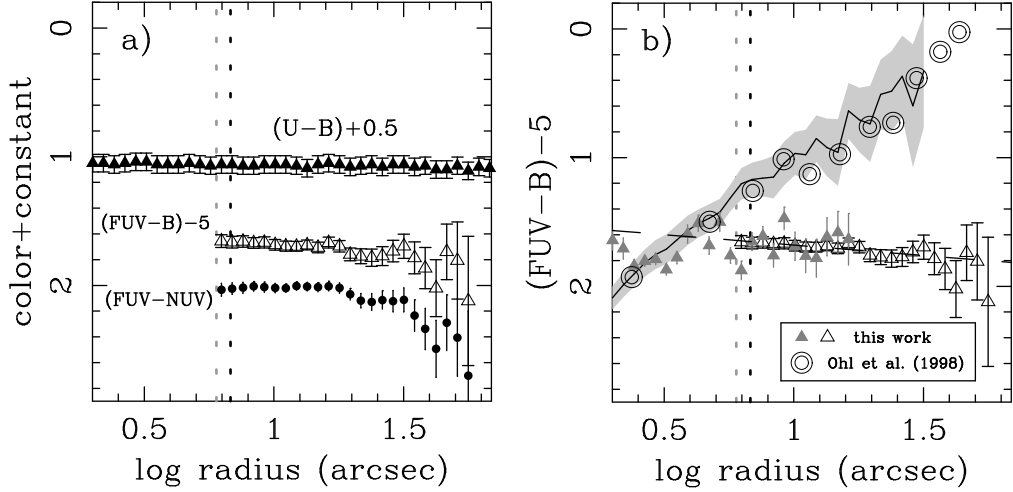


**FIGURE 4.** In Gil de Paz et al. [12] the luminosity profiles and color gradients have been derived for the compact elliptical galaxy M32, a nearby companion to Andromeda. The left panel shows that there is only a very slight color gradient in this galaxy which begins only in its outer regions, if at all. Surface photometry of this galaxy is especially difficult given that it is projected on the complex background of spiral structure in M31. The right-hand panel shows the divergence of photometry based on earlier photographic photometry (circles) and the GALEX observations (triangles).

and then by Ohl *et al.* [10] cast some doubt on M32 as being a truly typical elliptical galaxy. Based on UIT (Ultraviolet Imaging Telescope) data it was claimed that M32 had a strong FUV-optical color gradient, but that it was inverted (negative) with respect to the gradients observed in the vast majority of other elliptical galaxies. If true, M32 would be extremely anomalous. The imaging data for M32 had to be carefully decomposed so as to properly account for the complicated background contamination by the disk of M31. The results are shown in Figure 5 where it can be seen that M32 has a very modest (positive) color gradient making M32 fully consistent in its UV properties as compared to those observed in luminous ellipticals.

## M83: Extinction and Extended UV Disks

Boissier *et al.* [3] used FUV and NUV images of M83 to compute the radial profile of the UV spectral slope disk. They briefly present a model of its chemical evolution which allows them to obtain realistic intrinsic properties of the stellar populations. Using corollary data, they also compute the profiles of  $H\alpha/H\beta$  and of the total IR (TIR) to FUV ratio. Both data and model are used to estimate and compare the extinction gradients at the FUV wavelength obtained from these various indicators. They discuss the implications for the determination of the star formation rate.

Thilker *et al.* [14] have discovered an extensive sample of UV-bright stellar complexes in the extreme outer disk of M83 (Figure 6), extending four to five times the radius where the majority of  $H\text{ II}$  regions are detected ( $R_{H\text{ II}} = 5.1$  arcmin or 6.6 kpc). These sources are typically associated with large-scale filamentary  $H\text{ I}$  structures in the warped outer

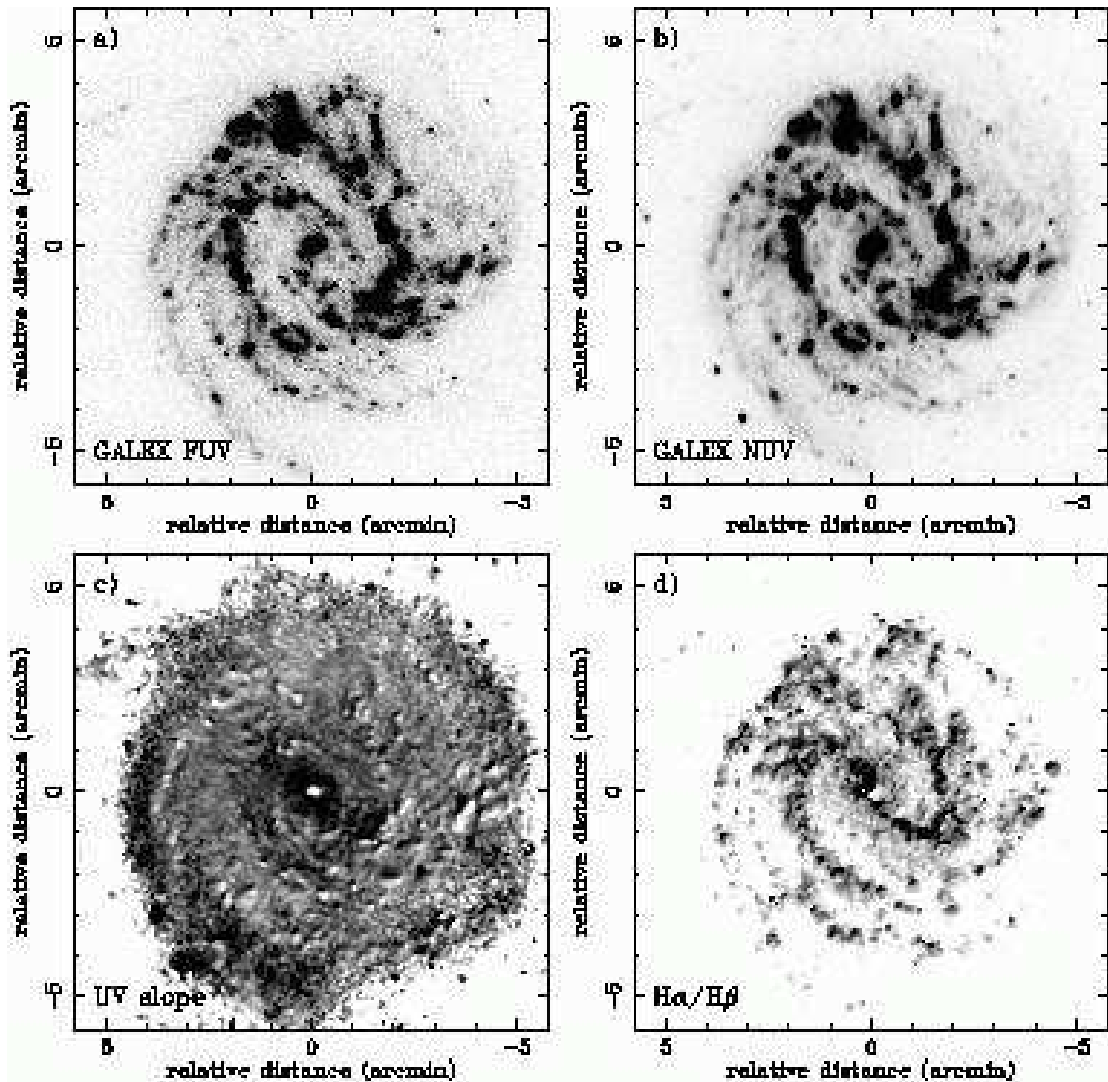


**FIGURE 5.** M83: (a) FUV image (from the sky background to 22.3 AB mag  $\text{arcsec}^{-2}$ ), (b) NUV image (from the sky background to 22.7 AB mag  $\text{arcsec}^{-2}$ ), (c) UV spectral slope, from  $-2.5$  (white) to  $0.3$  (black). (d)  $\text{H}\alpha/\text{H}\beta$  ratio, from  $\text{H}\alpha/\text{H}\beta=2$  to  $6$ . White areas in this plot correspond to regions where either  $\text{H}\alpha$  or  $\text{H}\beta$  was below  $3 \sigma_{\text{sky}}$ .  $8'' \times 8''$  median filters were applied in the case of panels (c) & (d). (Taken from Boissier *et al.* [3])

disk of M83, and are distributed beyond the galactocentric radii at which molecular ISM has yet been detected. It is of interest that only a subset of the outer disk UV sources have corresponding  $H\text{ II}$  regions detected in  $\text{H}\alpha$  imaging, consistent with a sample of mixed age in which a few sources are a few Myr old and the majority is much more evolved ( $\sim 10^8$  yr).

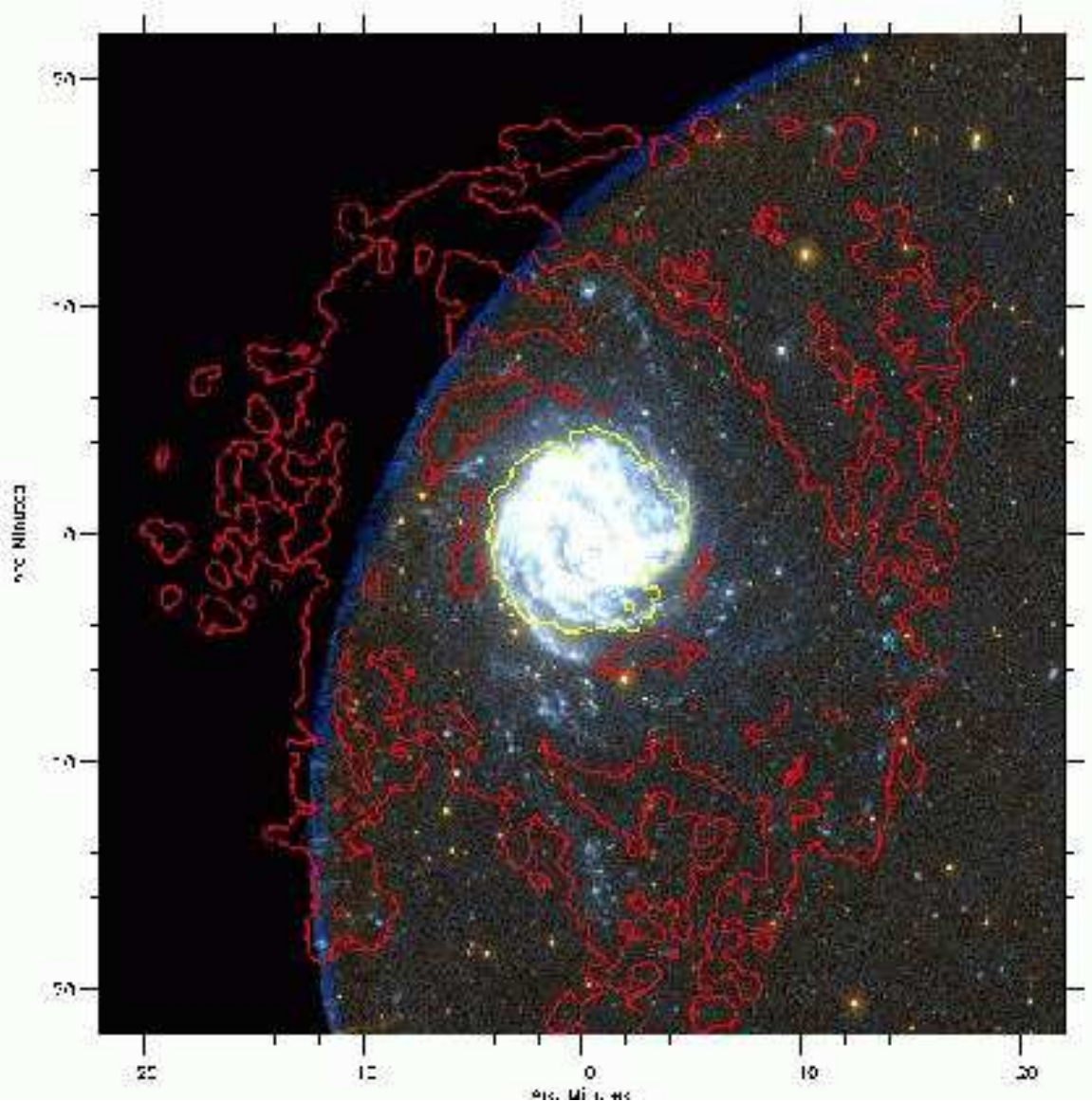


**FIGURE 6.** GALEX Imaging of M83. The grey-scale background image of M83 is derived from a combination of the FUV and NUV GALEX data. The contours correspond to the HI distribution published by Tilanus & Allen (1993) extend out to the limits of the image (44 arcmin diameter, which corresponds to a physical extent of about 60 kpc at the distance of M83; the inner disk of M83 as defined by its inner high-surface-brightness disk HII regions is about 5 times smaller (from Thilker *et al.* [14].

### M101: UV Leakage and Recent Star Formation

A comparative study of the spatial distribution of UV and far-infrared fluxes across the disk of M 101 has been undertaken by Popescu *et al.* [11]. By comparing total UV emission from both GALEX bands with total far-infrared (FIR) flux from ISOPHOT (60, 100 and 170  $\mu$ m) they discovered a very strong correspondence of the FIR/UV ratio with galactocentric radius (Figure 7). The ratio decreases monotonically from values

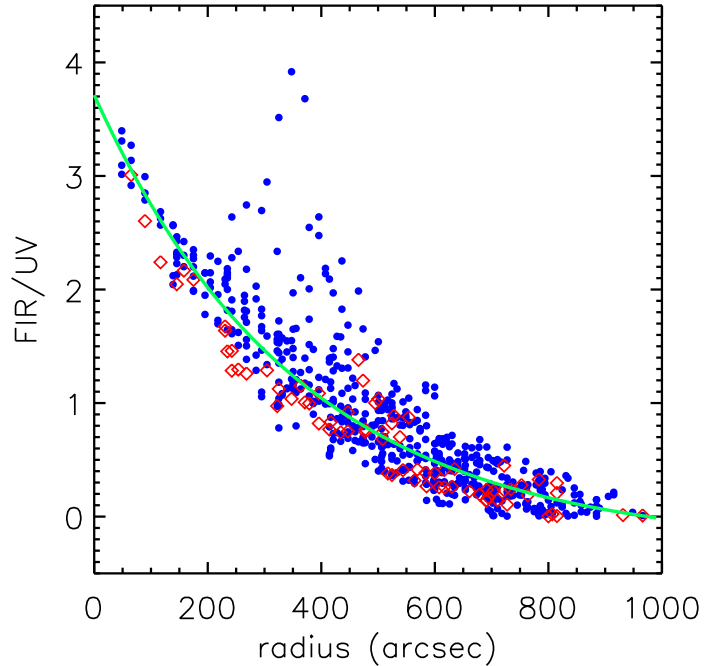


**FIGURE 7.** The pixel values of the FIR/UV ratio map of M101 at the resolution of the  $170\mu\text{m}$  image versus the galactocentric radius. The dots are for lines of sight towards interarm regions and the diamonds are towards the spiral arm regions. The solid line is an offset exponential fit to the data. (Adapted from Popescu *et al.* [11])

somewhat in excess of 3 near the nucleus to values near zero in the outer regions of the galaxy. This they attribute to a large-scale distribution of diffuse dust decreasing in optical depth with radius and dominating over the more localized variations in opacity occurring between the arm and interarm regions. They also find a tendency for the FIR/UV ratio (at a given radius) to take on higher values in the regions of diffuse interarm emission and lower values in the spiral-arm regions. This is interpreted both in terms of the escape probability of UV photons from spiral arms and their subsequent scattering in the interarm regions, and in terms of the larger relative contribution of optical photons to the heating of the dust in the interarm regions.

Another trend with galactocentric radius in M101 (and M51) is reported and discussed by Bianchi *et al.* [2]. Using GALEX and SDSS photometry of compact stellar clusters in M101 they have used population synthesis models to derive ages, reddenings luminosities and current/initial masses. A galactocentric gradient in the FUV/NUV color index suggests younger clusters are preferentially found in the outer parts of the disks, with M101 showing the more pronounced gradient as compared to M51. The radial profiles in FUV/NUV for other galaxies (M31, M33 and M83) show the same trend; however, the magnitude of the effect is variable from galaxy to galaxy.

## Interacting Galaxies and Tidal tails

Neff *et al.* [8] report the detection of significant FUV and NUV emission from stellar substructures within the tidal tails of four on-going galaxy mergers: ARP 157, ARP 295, NGC 5713/19 and NGC 7769/71. The UV-bright regions are optically faint and are coincident with *HI* density enhancements. FUV emission is detected at any location where the *HI* surface density exceeds  $\sim 2 \text{ M}_\odot \text{ pc}^{-2}$ , and is often detected in the absence of any visible wavelength emission. One example of UV tails and bridges, taken from their paper, is shown in Figure 8. UV luminosities of the brighter regions of the tidal tails imply masses of  $10^6 \text{ M}_\odot$  up to  $\sim 10^9 \text{ M}_\odot$  in young stars in the tails, and *HI* luminosities imply similar *HI* masses. UV-optical colors of the tidal tails indicate stellar populations as young as a few Myr, and in all cases ages  $< 400 \text{ Myr}$ . Most of the young stars in the tails formed in single bursts rather than resulting from continuous star formation, and they formed *in situ* as the tails evolved. Star formation appears to be older near the parent galaxies and younger at increasing distances from the parent galaxy. The youngest stellar concentrations, usually near the ends of long tidal tails, have masses comparable to confirmed tidal dwarf galaxies and may be newly forming galaxies undergoing their first burst of star formation.

A more detailed study of GALEX observations of an interacting galaxy, the Antennae, has been undertaken by Hibbard *et al.* [4]. The tidal *UV* morphology seen there is remarkably similar to the tidal neutral hydrogen gas, with a close correspondence between regions of bright *UV* emission and high *HI* column density. There are interesting features in the *UV* morphology of the inner regions. The *FUV* light in the south-western half of the disk of NGC 4039 is sharply truncated, coincident with a similar truncation in the *HI* disk. This gas may have been removed by the X-ray loops recently imaged in this system by *Chandra*, inhibiting subsequent star formation. On a larger scale, there is a *FUV* “halo”, possibly related to shocked gas in the X-ray halo.

While it has long been known that tails are generally blue, the GALEX observation provide color baselines to determine how much of the *UV* radiation comes from stars younger than the dynamical age of the tails. The preliminary analysis by Hibbard *et al.* [4] suggests that most of the stars within the tidal tails pre-date the tail formation period. The population in the northern tail appears older than that in the southern tail. Examining individual *UV*-bright regions within the tails they find regions of more recent star formation, which occur at regions of higher *HI* column density, and extend well beyond the previously identified tail star forming regions. Such tails are providing promising laboratories for the study of star formation outside of the usual disk environment, and thereby testing general theories of star and cluster formation.

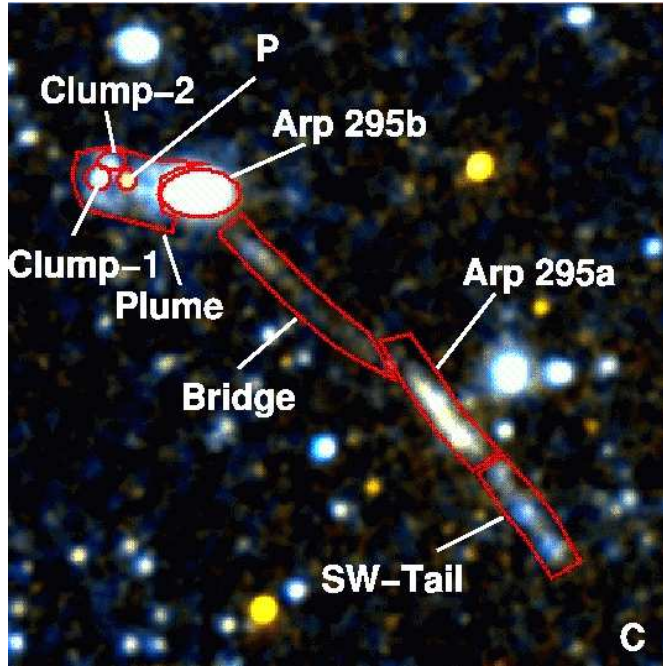


**FIGURE 8.** An example of the tidal tails discussed in Neff *et al.* [8]. In this case, the interacting system Arp 295 nicely illustrates the UV clumps, tails and bridges being found by GALEX in the outer regions of merging systems.

## ACKNOWLEDGMENTS

I want to thank Cristina Popescu and Richard Tuffs for the opportunity to report at their meeting on early results from the GALEX mission. And I thank all of my colleagues on the GALEX science team for their contributions to this interim review in specific and to the overall scientific success of the mission to date. I have shamelessly begged, borrowed and stolen images, plots, ideas and text from the many papers so far published by the Team; I hope that proper attribution is evident in this overview. A complete collection of papers resulting from the first round of publishing by the GALEX Team are slated to appear in a dedicated volume of the *Astrophysical Journal (Letters)* early in 2005; and they can also be found in their entirety at <http://www.galex.caltech.edu/PUBLICATIONS/>

The entire GALEX Team gratefully acknowledges NASA's support for construction, operation, and science analysis for the GALEX mission, developed in corporation with the Centre National d'Etudes Spatiales of France and the Korean Ministry of Science and Technology. The grism, imaging window, and uncoated aspheric corrector were supplied by France. We acknowledge the dedicated team of engineers, technicians, and administrative staff from JPL/Caltech, Orbital Sciences Corporation, University of California, Berkeley, Laboratoire Astrophysique Marseille, and the other institutions who made this mission possible. BFM was supported by the Observatories of Carnegie Institution of Washington and by the NASA/IPAC Extragalactic Database (NED).

## REFERENCES

1. Bianchi, L., *et al.* 2005a, ApJ 619, L27
2. Bianchi, L., *et al.* 2005b, ApJ 619, L71
3. Boissier, S., *et al.* 2005, ApJ 619, L83
4. Hibbard, J., *et al.* 2005, ApJ 619, L87
5. Hoopes, C.G., *et al.* 2005, ApJ 619, L99
6. Martin, D.C. *et al.* 2005, ApJ 619 L1
7. Morrissey, P., *et al.* 2005, ApJ 619, L7
8. Neff, S., *et al.* 2005, ApJ 619, L91
9. O'Connell, R. W., *et al.* 1992, ApJ, 395, L45
10. Ohl, R. G., *et al.* 1998, ApJ, 505, L11
11. Popescu, C.C., *et al.* 2005, ApJ 619, L75
12. Gil de Paz, A., *et al.* 2005, ApJ 619, L115
13. Thilker, D.A., *et al.* 2005a, ApJ 619, L67
14. Thilker, D.A., *et al.* 2005b, ApJ 619, L79
15. Tilanius, R.P.J., & Allen, R.J. 1993, A & Ap, 274, 707